University of Bath

Alternative formats
If you require this document in an alternative format, please contact:
openaccess@bath.ac.uk

Skin pharmacokinetics of transdermal scopolamine: measurements and modelling

*Andrea Pensado[1, †], Laura Hattam[2], K.A. Jane White[3], Anita McGrogan[1], Annette L. Bunge[4], Richard H. Guy[1], M. Begoña Delgado-Charro[1, *]*

[1] Department of Pharmacy & Pharmacology, University of Bath, Bath, BA2 7AY, UK

[2] Institute for Mathematical Innovation, University of Bath, Bath, BA2 7AY, UK

[3] Department of Mathematical Sciences, University of Bath, Bath, BA2 7AY, UK

[4] Chemical and Biological Engineering, Colorado School of Mines, Golden, Colorado, 80401,USA

AUTHOR INFORMATION

[*] **Corresponding Author**

M. Begoña Delgado-Charro. Department of Pharmacy and Pharmacology, University of Bath,

Claverton Down, Bath, BA2 7AY, UK. Phone: 44 1225 383969. B.Delgado-Charro@bath.ac.uk

[†] **Present Addresses**

R&D Cluster Programs Section, Okinawa Institute for Science and Technology, Technology

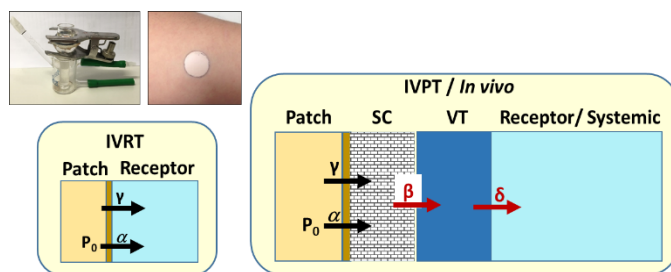Development and Innovation Center, Japan. andrea.pensadolopez@oist.jp.

Declarations of interest: None

For Table of Contents Use Only

Skin pharmacokinetics of transdermal scopolamine: measurements and modelling

Andrea Pensado, Laura Hattam, K.A. Jane White, Anita McGrogan, Annette L. Bunge,

Richard H. Guy, M. Begoña Delgado-Charro

ABSTRACT

Prediction of skin absorption and local bioavailability from topical formulations remains a difficult task. An important challenge in forecasting topical bioavailability is the limited information available about local and systemic drug concentrations post-application of topical drug products. Commercially available transdermal patches, such as Scopoderm® (Novartis Consumer Health UK), offer an opportunity to test these experimental approaches as systemic pharmacokinetic data is available with which to validate a predictive model. The long-term research aim, therefore, is to develop a physiologically-based pharmacokinetic model (PBPK) to predict the dermal absorption and disposition of actives included in complex dermatological products. This work explored whether *in vitro* release and skin permeation tests (IVRT and IVPT, respectively), and *in vitro* and *in vivo* stratum corneum (SC) and viable tissue (VT) sampling data, can provide a satisfactory description of drug "input rate" into the skin and subsequently into the systemic circulation. *In vitro* release and skin permeation results for scopolamine were consistent with the previously reported performance of the commercial patch investigated. New skin sampling data on the dermatopharmacokinetics (DPK) of scopolamine also reflected accurately the rapid delivery of a "priming" dose from the patch adhesive, superimposed on a slower, rate-controlled input from the drug reservoir. The scopolamine concentration versus time profiles in SC and VT skin compartments, *in vitro* and *in vivo*, taken together with IVRT release and IVPT penetration kinetics, reflect the input rate and drug delivery specifications of the Scopoderm® transdermal patch and reveal the importance of skin binding with respect to local drug disposition. Further data analysis and skin PK modelling are indicated to further refine and develop the approach outlined.

KEYWORDS: topical drug bioavailability; skin pharmacokinetics; *in vitro* release test; *in vitro* skin permeation; DPK modelling, scopolamine

INTRODUCTION

The local pharmacokinetics of topically applied drugs in the skin (also known as dermatopharmacokinetics or DPK) have proven difficult to characterize quantitatively. This is primarily due to the fact that the measurement of drug levels in the relevant skin tissues is experimentally challenging. In addition, the systemic circulation has not generally been considered an appropriate "surrogate" compartment for the skin, either because of concerns that blood levels do not usefully inform DPK, or due simply to difficulties in quantifying the drug itself [1-3].

Nonetheless, the need for information about DPK remains acute for the development of topical medicines to treat disease targets in the skin. Knowledge of whether a therapeutic concentration of the drug at its site of action in, for example, the basal epidermis, is essential for efficient formulation development and for the design of an appropriate dosage regimen. Equally, the availability of methodological tools, with which to characterize DPK, is necessary to provide sensible metrics for the assessment of local bioavailability and bioequivalence and, thereby, to enable generic products to be approved without the need for clinical end-point studies [3,4].

To address the objective of drug disposition in the skin following topical administration, the classic pharmacokinetic (PK) processes of absorption, distribution, metabolism and excretion (i.e., ADME) must obviously be considered. Although metabolic activity in the skin is recognized (particularly that of esterases), drug biotransformation is in general at best a secondary phenomenon of likely significance in only a few instances [5]. With respect to distribution, there are two important phenomena to be considered. First, the stratum corneum (SC), the skin's outer layer and principal barrier, is known to provide an environment where lipophilic drugs, in particular, can be "waylaid", forming what is sometimes referred to as a reservoir; this may involve passive

partitioning and/or a more specific binding to the abundant keratin in the corneocytes [6,7]. Second, once drug reaches the living skin below the SC, more conventional protein binding can occur, presumably in a manner not too dissimilar to that occurring systemically [8,9].

There remains, then, the two key PK processes of absorption and elimination. The literature includes multiple investigations into the phenomenon of drug clearance from the viable skin, and a number of predictive models have been proposed [10,11]. It is well-accepted that diffusion in the living tissue is rapid compared to that through the SC, ensuring therefore a relatively small decrease in drug concentration from the SC-viable tissue interface to the rich plexus of microcirculation in the upper dermis that guarantees the eventual removal of drug into the systemic circulation [10,12]. Self-evidently, it is the balance between this clearance and drug input via drug absorption into and permeation through the SC which determines, therefore, the DPK profile in the skin of a topically absorbed drug and quantification of these processes is essential to assess whether a particular medicine will be therapeutically effective or not.

Recently, the components of drug DPK have received increased attention. For example, *in vitro* skin permeation tests (IVPT), supplemented by simpler *in vitro* release testing (IVRT) of formulations in the absence of skin, have been subjected to detailed investigation [13,14], SC sampling by adhesive tape stripping (*in vivo* and *in vitro*) has shown that drug input into the viable epidermis can be deduced via careful protocol design [15,16], and open-flow microperfusion is now providing direct and high-quality *in vivo* measurements of drug PK profiles in the dermis [17]. An important challenge that remains, however, is validation of the different methodologies and correlation between *in vitro* and *in vivo* approaches. Of particular significance, furthermore, is the fact that post-application changes in the complicated compositional and structural properties of topical drug products impose substantial demands on models that attempt to faithfully simulate the subsequent

6

disposition kinetics of the active in the skin. For this challenge to be met, drug input at the formulation-SC interface must be understood better and fully characterised by dermatopharmacokinetic (DPK) measurements.

Here, a combination of IVRT, IVPT and SC sampling *in vitro* and *in vivo* is used to assess the dermal disposition and penetration of scopolamine from a commercially available system (Scopoderm®, Novartis Consumer Health) designed to be worn for 72 hr. This product, which is closely similar to the first patch that was approved over 40 years ago, is a multilaminate system formed of 4 layers: (a) an adhesive layer that sticks to the skin and contains scopolamine in a polymeric gel which provides an initial priming dose; (b) an intermediate microporous polypropylene rate-controlling membrane; (c) the scopolamine reservoir that sustains a zero-order input of drug to the skin surface, and (d) a backing of impermeable aluminized polyester film. It follows that the patch has a very well-understood mechanism of drug input to the skin surface [18-20], thereby "fixing" the absorption component of DPK and enabling the subsequent penetration profile and disposition of the drug into the deeper layers of the skin to be fully characterized.

MATERIALS & METHODS

Materials

Scopoderm® 1.5 mg patches (2.5 cm^2) (Novartis Consumer Health UK Limited, Camberley, UK) were acquired through the departmental pharmacy (University of Bath, Department of Pharmacy & Pharmacology). Pure scopolamine hydrobromide, solvents and HPLC reagents were from Sigma Aldrich (Gillingham, UK).

Excised abdominal pig skin (from a single animal) was obtained from a local abattoir; to preserve the integrity of the skin barrier, the skin was not exposed to the normal high-temperature cleaning procedure. Skin was washed with water, dermatomed (Zimmer®, Hudson, OH, USA), to a nominal thickness of 750 µm, frozen within 24 h of slaughter, and thawed before use.

Methods

In vitro release test (IVRT)

The release of scopolamine from the transdermal therapeutic system was evaluated using side-by-side diffusion cells. The Scopoderm® patches (area = 2.5 cm^2) were placed between the two half-cells creating a 1.23 cm^2 area of transport). The receptor chamber was filled with 4 mL of phosphate-buffered saline (pH 7.4) and magnetically stirred. The entire experiment was performed in an oven at 32°C, except for brief periods (of less than a minute) when the receptor solution was sampled at 1, 2, 4, 6, 8, 10, 24, 48 and 72 h. Aliquots (1 mL) withdrawn from the receptor were replaced with the same volume of fresh receptor solution. Receptor samples were filtered (Cronus syringe filter, nylon, 4 mm, 0.45 µm, LabHut, UK) and the concentration of scopolamine in the samples was quantified using HPLC-UV.

Data were expressed as the cumulative scopolamine released per unit area (µg cm^{-2}) and as the corresponding flux, i.e., amount of scopolamine released per unit area per unit time (µg cm^{-2} h^{-1}) in each sampling interval. The apparent steady-state flux between 24 and 72 h was calculated from the slope of the linear regression (GraphPad Prism 5.00, GraphPad Software, San Diego, USA) of the cumulative amount of scopolamine released versus time over this period.

In vitro skin permeation test (IVPT)

The Scopoderm® patch was adhered to excised abdominal porcine skin, which was positioned on (and slightly overlapped) a vertical Franz diffusion cell (PermeGear, Inc., Bethlehem, USA) so that the skin area of transport from the patch was 2.5 cm². The dermal side of the skin was bathed by the pH 7.4 phosphate-buffered saline receptor medium (7.4 mL) which was magnetically stirred. The duration of the experiment was 72 h. Climate control, receptor solution sampling, and data analysis mirrored those of the IVRT experiments.

In vitro SC and 'viable' tissue (VT) sampling

Scopolamine uptake into the SC following patch application was determined in a separate set of IVPT experiments. After uptake times of 2, 4, 6, 8, 10, 24, 48, and 72 h (during which periods receptor solution sampling was performed as possible), the diffusion cell was dismantled and the SC was removed by repeated tape stripping (Scotch Book Tape, 3M, The Consortium, UK): adhesive tape strips (2.5 x 2.5 cm²) were applied to the skin, pressed down firmly, and then removed in alternating directions for up to 30 strips; the glistening appearance of the skin surface made it visually clear when the SC had been fully removed and this was typically achieved after 20 strips. For analysis of the drug in the SC, the tape-strips were grouped (numbers 1-5, 6-10, 11-20, and 21-30) to ensure sufficient assay sensitivity. Scopolamine was efficiently extracted (95%) from the groups of tape strips with 3.5 mL of 30:70 methanol:water and sonication for 0.75 h at 40°C. After tape stripping the SC, the amount of scopolamine in the remaining epidermis plus dermis (i.e., the VT) was also measured. For this, the drug was extracted by shaking the remaining tissue overnight with 3.5 mL of 30:70 methanol:water. Extract samples from the tape strips and VT were filtered (Cronus syringe filter, nylon, 4 mm, 0.45 μm, LabHut, UK), transferred to 2-ml HPLC vials, and scopolamine was quantified by HPLC as described below.

A further set of experiments investigated the rate at which the drug was cleared from the SC and VT. The scopolamine patch was applied to the skin for 4 h and then gently removed. In a series of experiments, drug in the SC and VT was subsequently assessed (in the same way as described above) immediately after uptake and then following four periods of 'clearance' (2, 3, 4 and 20 h).

In vivo SC sampling

The study was approved by the Research Ethics Approval Committee for Health at the University of Bath (REACH EP 16/17 223). Six healthy volunteers (3 female, 3 male; mean ($\pm$SD) age: 28 ($\pm$ 3) years) participated in the study having given informed consent. For subjects with significant hair on the forearms, the skin was shaved using a new disposable razor at least 24 h before the study. No lotion, cream or other personal care product was used on the test sites for at least 24 h before or during the study.

One hour before patch application, the forearm to be treated was washed with a mild soap solution (Carex Complete, Cussons, Manchester, UK) and allowed to dry. From the same forearm, but at a distant site, a few tape strips were collected to provide drug-free samples of SC as controls for the analytical method. Transepidermal water loss (TEWL) rate was measured (AquaFlux, Biox Systems Ltd., London, UK) at the skin site to be treated, providing a baseline (i.e., untreated, unstripped skin) value. The protocol employed closely followed previous *in vivo* studies of econazole, acyclovir and diclofenac topical products [15,16,21]; specifically, the mass of drug in the SC was measured after the 4-h 'uptake' period and at two 'clearance' times, 3 and 20 h later. Uptake and clearance times were staggered so that each subject only had one patch applied at any given time and such that the total time of patch-wear (12 h) was only 16% of the labelled, approved exposure period of the patch (72h). All patches were applied to the same arm. A schematic of the

experimental protocol is provided in Figure S1 in the Supplementary Information. After each patch removal, the skin site was cleaned with a 70% isopropyl alcohol wipe (Sterets®, Molnlycke, Lancashire, UK). Templates (Scotch® Book Tape, 3M, St. Paul, MN, USA), with an opening of 1.54 cm^2 that controlled the skin stripping area, were prepared and affixed to the treated sites. SC at the 'uptake' site was tape-stripped immediately after cleaning. The two clearance sites were demarcated using Mefix® tape (Molnlycke, Lancashire, UK) and covered with light gauze (Boots, Nottingham, UK) to protect the sites; then, at the designated times, the gauze was removed, and the SC was sampled.

The SC sampling and analysis procedure was same as that used *in vitro*. To ensure that a significant fraction of the SC was removed by the tape-stripping procedure without too much discomfort for the volunteers [21], TEWL was measured intermittently during tape-stripping [22, 23] until either (i) its value reached 60 g m^{-2} h^{-1}, or was ≥6-times the baseline, pre-treatment control, or (ii) 30 tape-strips had been removed.

HPLC Analysis

Scopolamine samples were quantified by HPLC with UV detection at 210 nm (Shimadzu LC-2010, Buckinghamshire, UK) using a 5-mm Eclipse XDB Cyano Column (250 x 4.6 mm) (Agilent Technologies, Stockport, UK). The mobile phase comprised a 68:32 mixture of (A) 20% acetonitrile in 20 mM, pH 6 phosphate buffer, and (B) acetonitrile. The flow rate was 1 mLmin^{-1}, the injection volume 50 µL, and the drug retention time was ~5 minutes. The limits of quantification (LOQ) and detection (LOD) for scopolamine in the extraction solvent (30:70 methanol:water) were 0.16 and 0.05 µg mL^{-1}, respectively, corresponding to 0.051 and 0.008 µg cm^{-2} for the tape strips, and 0.079 and 0.013 µg cm^{-2} for the VT. In PBS, the LOQ and LOD were

0.45 and 0.13 µg mL^{-1}, respectively. Any measurement less than the relevant LOQ was assigned the value of zero.

Data analysis

Statistically significant differences were estimated by a two-tail t-test or by one-way ANOVA followed by Tukey's test (GraphPad Prism 5.00, GraphPad Software, San Diego, USA). In all the comparisons undertaken, statistical significance was set at $p < 0.05$. The Grubbs' Test was performed to detect significant outlier values. Reported 95% confidence intervals were calculated using the two-tailed Student's t-distribution of a probability of 0.05 for the sample size and standard deviation.

The total *in vitro* scopolamine uptake into the skin, designated as IVPT (M+V+R), was calculated by summing the average drug amounts measured in the SC (M), VT (V) and receptor (R) at each sampling time. The variance of IVPT (M+V+R) was estimated as the sum of the variances for the independent measurements of drug amounts in each of these compartments. Because the number of replicates (n) in the SC, VT and the receptor at each sampling time varied, confidence intervals were calculated using the smallest n for the SC, VT and receptor; in most cases n = 3. The confidence intervals reported for IVPT (M+V+R) should therefore tend toward a conservative (i.e., maximized) estimate. The estimated confidence intervals for the IVPT (M+V+R) flux at each time point were derived from the variances in the receptor flux and drug amounts determined in the SC and VT combined. Variance in the drug flux into the SC and VT was estimated from the sum of the variances in the drug mass at the start and end time points of the flux time interval. (See Supplementary Information for details.)

Mathematical modelling

The IVPT experimental data (including tape-stripping) were analyzed using the mathematical model presented schematically in Figure 1, in which the transfers of drug mass per area from the SC (M) to the VT (V), and from the VT to the receptor fluid (R), are represented by the first-order rate constants β and δ, respectively. The IVRT experiments were described by a comparable model that contains only the receptor fluid compartment. Drug flux from the patch (J_{patch}) is modeled by a steady-state rate (γ) combined with a priming dose (P_0) that depletes with a first-order rate constant α [20]. Table 1 lists the equations that define, for both the IVPT and IVRT systems, the time rate of change of the drug mass per area in each compartment, as well as the drug mass per area in each compartment at time t and at steady state for the IVRT experiments. Separate equations describe the IVPT experiments during drug uptake from the patch and drug clearance from the skin after the patch is removed.
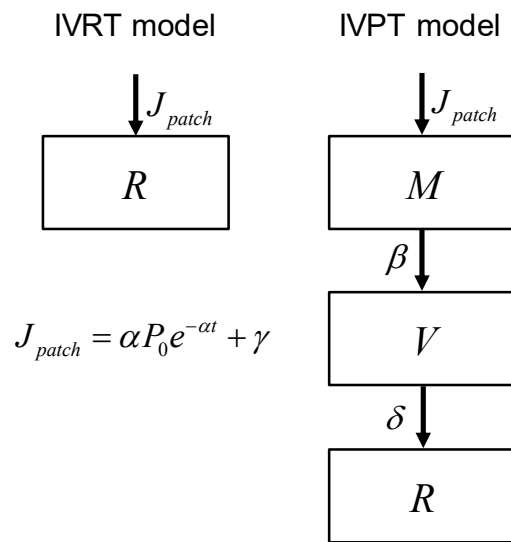

Figure 1. Schematic diagrams of the pharmacokinetic (compartment) models describing the IVRT and IVPT (including stratum corneum and viable tissue sampling) experiments during uptake, where M, V and R represent respectively the drug mass per area in the SC, the VT and the receptor

13

fluid compartments, α, β, and δ are first-order rate constants, and γ is the zero-order, steady-state transfer rate from the patch. During clearance, $J_{patch} = 0$.

Parameters for models in Table 1 were determined as described below by best-fit regressions of experimental data to the appropriate equation using GraphPad Prism 5.00. Values for α, γ and P_0 were derived by best-fit regression of the mean values of the IVRT experimental data at each measurement time to the IVRT model (Eq. A) in Table 1. Because the skin might slow drug delivery from the patch, IVPT values for α and γ were derived by best-fit regression of the IVPT data to the IVPT model (Eq. C in Table 1) for the mean drug mass at each measurement time in the receptor (R) and in the skin and receptor combined (i.e., $M+V+R$) while keeping the mass per area of the priming dose (P_0) at the value determined from the IVRT experiment. Values for β and δ in the IVPT uptake model were calculated from the mean value of the experimental drug mass in the VT (V_{ss}) and the SC (M_{ss}) at 72 h, assumed to be at steady state, and the IVPT value of γ as specified by Eqs. D and E in Table 1. Best-fit parameter values were also derived from the clearance data by successively regressing the IVPT clearance model equations in Table 1 to the drug mass measured versus time in the SC to determine M_{up} and β (Eq. F), in the VT to determine V_{up} and δ (Eq. G), and in the receptor solution to determine R_{up} (Eq. H), where the subscript 'up' denotes the drug mass in the designated compartment at the end of the 'uptake' period.

Table 1. Pharmacokinetic model equations

Model	Compartment	Differential drug mass balance	Drug mass		Steady-state (*ss*) drug mass
IVRT [a]	Receptor (R)	$\dfrac{dR}{dt} = J_{patch}$	$R = P_0\left(1 - e^{-\alpha t}\right) + \gamma t$	(Eq. A)	$R_{ss} = P_0 + \gamma t$
IVPT – uptake [a,b] ($t \leq t_{up}$)	SC (M)	$\dfrac{dM}{dt} = J_{patch} - \beta M$	$M = \dfrac{\alpha P_0}{\alpha - \beta}\left(e^{-\beta t} - e^{-\alpha t}\right) + \dfrac{\gamma}{\beta}\left(1 - e^{-\beta t}\right)$		$M_{ss} = \dfrac{\gamma}{\beta}$ (Eq. D)
	VT (V)	$\dfrac{dV}{dt} = \beta M - \delta V$	$V = \dfrac{\alpha \beta P_0}{\alpha - \beta}\left(\dfrac{e^{-\delta t} - e^{-\alpha t}}{\delta - \alpha} - \dfrac{e^{-\delta t} - e^{-\beta t}}{\delta - \beta}\right)$ $+ \gamma\left(\dfrac{1 - e^{-\delta t}}{\delta} + \dfrac{e^{-\delta t} - e^{-\beta t}}{\delta - \beta}\right)$		$V_{ss} = \dfrac{\gamma}{\delta}$ (Eq. E)
	Receptor (R)	$\dfrac{dR}{dt} = \delta V$	$R = \dfrac{P_0}{\alpha - \beta}\left\{\dfrac{\beta}{\delta - \alpha}\left[\alpha\left(1 - e^{-\delta t}\right) - \delta\left(1 - e^{-\alpha t}\right)\right]\right.$ $\left. - \dfrac{\alpha}{\delta - \beta}\left[\beta\left(1 - e^{-\delta t}\right) - \delta\left(1 - e^{-\beta t}\right)\right]\right\}$ $+ \dfrac{\gamma}{\delta - \beta}\left[\left(1 - e^{-\delta t}\right) - \dfrac{\delta\left(1 - e^{-\beta t}\right)}{\beta}\right]$ $+ \gamma\left(t - \dfrac{1 - e^{-\delta t}}{\delta}\right)$ (Eq. B)		$R_{ss} = P_0 + \gamma t - M_{ss} - V_{ss}$ $= P_0 + \gamma t - \gamma\left(\dfrac{1}{\beta} + \dfrac{1}{\delta}\right)$
	All ($M + V + R$)	$\dfrac{d\left(M + V + R\right)}{dt} = J_{patch}$	$M + V + R = P_0\left(1 - e^{-\alpha t}\right) + \gamma t$	(Eq. C)	$M_{ss} + V_{ss} + R_{ss} = P_0 + \gamma t$
IVPT – clearance ($t > t_{up}$) [c]	SC (M_{cl})	$\dfrac{dM_{cl}}{dt} = -\beta M_{cl}$	$M_{cl} = M_{up}e^{-\beta\left(t - t_{up}\right)}$	(Eq. F)	$M_{cl,ss} = 0$
	VT (V_{cl})	$\dfrac{dV_{cl}}{dt} = \beta M_{cl} - \delta V_{cl}$	$V_{cl} = V_{up}e^{-\delta\left(t - t_{up}\right)}$ $- \dfrac{\beta M_{up}}{\beta - \delta}\left(e^{-\beta\left(t - t_{up}\right)} - e^{-\delta\left(t - t_{up}\right)}\right)$ (Eq. G)		$V_{cl,ss} = 0$

Receptor (R_{cl})	$\dfrac{dR_{cl}}{dt} = \delta V_{cl}$	$R_{cl} = R_{up} + V_{up}\left(1 - e^{-\delta(t-t_{up})}\right)$ $+ M_{up}\left(1 - \dfrac{\beta e^{-\delta(t-t_{up})} - \delta e^{-\beta(t-t_{up})}}{\beta - \delta}\right)$ (Eq. H)	$R_{cl,ss} = M_{up} + V_{up} + R_{up}$ $= P_0\left(1 - e^{-\alpha t_{up}}\right) + \gamma t_{up}$
All ($M_{cl} + V_{cl} + R_{cl}$)	$\dfrac{d(M_{cl} + V_{cl} + R_{cl})}{dt} = 0$	$M_{cl} + V_{cl} + R_{cl} = P_0\left(1 - e^{-\alpha t_{up}}\right) + \gamma t_{up}$	$M_{cl,ss} + V_{cl,ss} + R_{cl,ss}$ $= P_0\left(1 - e^{-\alpha t_{up}}\right) + \gamma t_{up}$

[a] Flux from the patch to the receptor solution or the skin ($J_{patch} = \alpha P_0 e^{-\alpha t} + \gamma$) includes transfer from the priming dose P_0 (mg/cm^2) at a rate described by the first-order rate constant α (h^{-1}) and steady-state transfer γ (mg/cm^2/h), which is assumed to continue during the entire time the patch is applied to the skin (i.e., $t \leq t_{Up}$).

[b] Equations describing the drug mass per area in the designated compartments at time t during uptake from the patch are derived by solving the differential drug mass balances using $R = 0$ at $t = 0$ for the IVRT model and $M = V = R = 0$ at $t = 0$ for the IVPT-uptake model [20].

[c] Equations describing the drug mass in the designated compartments at time t after the patch is removed (i.e., during clearance and $J_{patch} = 0$) are derived by solving the differential drug mass balances using $M_{cl} = M_{up}$, $V_{cl} = V_{up}$, and $R_{cl} = R_{up}$, at $t = t_{up}$ where M_{up}, V_{up}, and R_{up} are calculated from the IVPT-uptake equations at $t = t_{up}$.

RESULTS

1. IVRT and IVPT experiments:

The cumulative amounts per unit area of scopolamine (a) released directly from the patch (IVRT), and (b) delivered across porcine skin (IVPT (R)), into the receptor medium are plotted as a function of time in Figure 2(a). The IVRT data show a clear, initial 'burst' effect after which the rate of appearance of scopolamine in the receptor medium becomes constant. The profile for the IVPT experiment is similar but is 'delayed' by a period of about 4 h. Figure 2(b) replots the IVRT and IVPT cumulative appearances in the receptor phase in terms of drug flux as a function of time. As can be inferred from Figure 2(a), drug flux in the IVRT experiment is initially very high but then decreases quite quickly to a low and steady value. In the IVPT study, in contrast, drug flux increases after a short lag period to around 6 to 8 h before falling to a lower and steady value that is a little smaller than that observed in the IVRT experiment. Parameter values for the model predictions shown in Figure 2 are listed in Table 2 and described below.
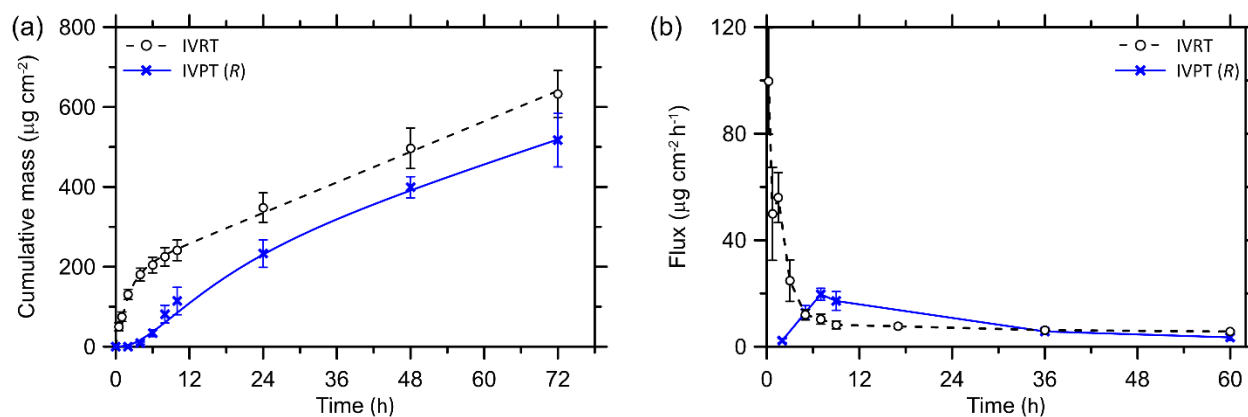

Figure 2. (a) Cumulative scopolamine released per unit area in IVRT and delivered per unit area across porcine skin (IVPT (R)), *in vitro* as a function of time. Data points represent the mean and 95% confidence interval (CI) (n = 7 for IVRT; n = 6 for IVPT (R) except at 2 h (n = 5), 4 h (n = 22), 6 h (n = 14), and 10 h (n = 3)); no drug was detectable in IVPT (R) at 2 h. For both profiles,

the lines drawn through the data represent the predictions of the IVRT and IVPT uptake models in

Table 1 with parameters derived by best-fit regression to the drug released from the patch in the

presence and absence of skin (see Table 2). (b) Scopolamine flux per unit area into the receptor

fluid in the IVRT and IVPT (R) experiments as a function of time. Fluxes were calculated from

successive pairs of data in Figure 2(a), and plotted at the mid-point of the sampling times (except

for the flux plotted at 2 h, which is the average flux for the 0-4 h time interval and there is no flux

plotted at 17 h for the 10-24 h time interval because both times were not measured in the same

experiment). Values are the mean ± 95% CI (n = 7 for IVRT; n = 3 or 4 for IVPT (R) except at 2

h (n = 22), 5 h (n = 14), and 7 h (n = 6)).

Table 2. Mathematical model parameter values derived by regression to IVRT and IVPT data

Experiment	P_0 (µg cm^{-2})	α (h^{-1})	γ (h^{-1})	β (h^{-1})	δ (h^{-1})	$M_{ss}{}^{a}$ (µg cm^{-2})	$V_{ss}{}^{a}$ (µg cm^{-2})		
IVRT	182	0.49	6.4						
IVPT uptake (M+V+R)	182^{b}	0.07	5.0	1.1	0.25	20.1	4.7		
						M_{up} (µg cm^{-2})	V_{up} (µg cm^{-2})	R_{up} (µg cm^{-2})	$M_{up} + V_{up} + R_{up}$ (µg cm^{-2})
IVPT clearance				0.04	0.21	25.6	10.9	20.3	56.8

^{a} Measurement at 72 h assumed to be at steady state
^{b} Set to the best-fit value for the IVRT uptake data.

2. Stratum corneum (SC) and 'viable' tissue (VT) sampling:

In vitro drug uptake measurements into the skin were performed in separate experiments at the

same time points that receptor phase samples were acquired in the IVPT study. Scopolamine was quantified in both the SC and VT and the results, expressed in terms of drug amount per unit area of skin, are presented in Figure 3. The quantity of drug in the SC rapidly reached about 40 µg cm^{-2} and remained at this level for ~6 h. Thereafter, the amount in the SC decreased to a fairly constant level of 5 µg cm^{-2} over what would correspond to the second half of a period of normal patch wear, i.e., 36-72 h post-application. In contrast, the scopolamine level in the VT rose somewhat less quickly reaching a maximum after about 8 h of patch application, and thereafter remained essentially constant at ~20 µg cm^{-2}. The amounts of drug recovered in the SC and VT plus the cumulative quantity in the receptor at the corresponding time points, identified as IVPT (M+V+R), are compared in Figure 3(b) with drug release from the patch in the absence of skin (IVRT), replotted from Figure 2(a).
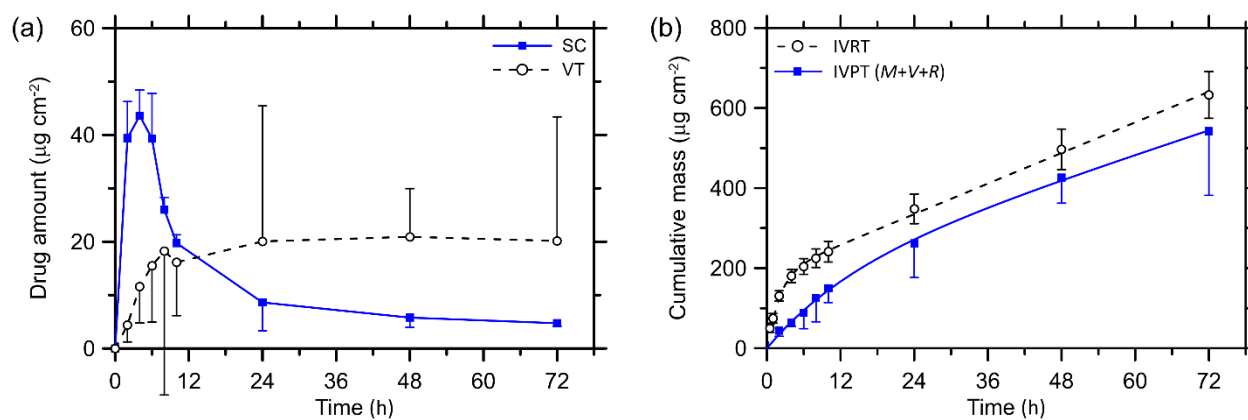

Figure 3. (a) Amount of scopolamine recovered per unit area from the SC and the VT following application of a transdermal patch *in vitro* for different times. Values are the mean and 95% CI (n = 3 except at 2 h (n = 5 for SC) and 4 h (n = 11 for SC and n = 9 for VT)). (b) Cumulative drug delivered across the skin to the receptor plus the quantities in the skin (i.e., SC+VT), again as a function of time (IVPT (M+V+R), compared with the cumulative drug release from the patch in the absence of skin (IVRT) from Figure 2(a). Data represent the mean and 95% CI calculated for

IVRT using n = 7, and for IVPT (M+V+R) using n = 3, except at 4 h (n = 9); see Methods). The lines drawn through the data represents the best-fit regression to the IVRT and IVPT (*M+V+R*) models in Table 1 (see Table 2).

A subsequent set of *in vitro* experiments was designed to assess scopolamine clearance from the skin (both SC and VT) after patch removal. The transdermal systems were applied for an 'uptake' period of 4 h and drug amounts in the SC and VT were determined either immediately upon removal or following 2, 3, 4 and 20 h of 'clearance'; scopolamine, which had permeated all the way to the receptor phase, was also quantified at 'uptake' and at all 'clearance' times. The results are shown in Figure 4. There was no significant difference (one-way ANOVA) in the total quantities of drug recovered (SC+VT+Receptor) at the different times. There was, however, a monotonic decrease in the amount of scopolamine in both the SC and the VT during 'clearance' (i.e., post-removal of the patch). On assumption that drug clearance from the SC and VT followed first-order kinetics, the rate constants for elimination from the SC to the VT and from the VT to the receptor were 0.04 ($\pm$ 0.01) h^{-1} and 0.05 ($\pm$ 0.01) h^{-1}.

Finally, SC sampling was performed *in vivo*, with a 4-h 'uptake' period and two 'clearance' periods of 3 and 20 h. The results are shown in Figure 5 and are compared with those (discussed above) obtained *in vitro* for the SC and for the VT. The SC profiles *in vivo* and *in vitro* are in good agreement and there were no statistically significant differences between the values measured at 'uptake' or between those assessed in 'clearance' at either 3 or 20 h. With the same assumption that drug clearance from the SC to the VT also follows first-order kinetics, the rate constant *in vivo* was determined to be 0.03 ($\pm$ 0.02) h^{-1}. The 'clearance' profile from the VT mirrored that from

the SC (*in vitro* and *in vivo*); this indicates that drug removal from the VT is rate-controlled by its slow input from the SC.
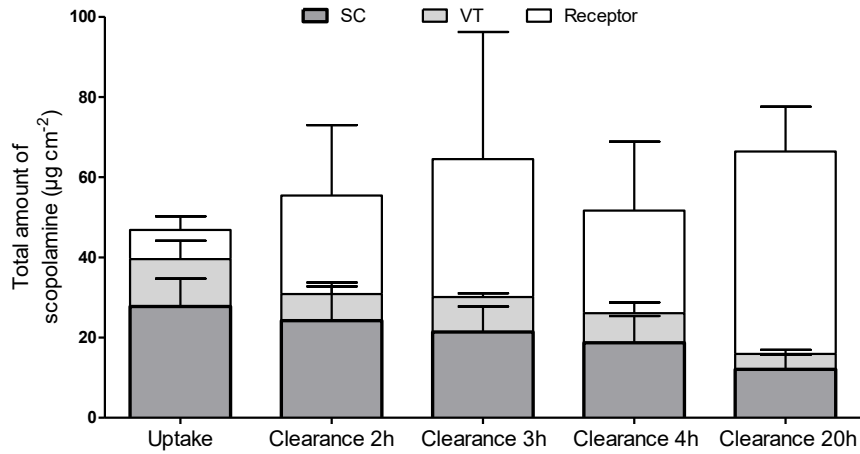

Figure 4. Scopolamine recovered per unit area from the SC, VT and receptor compartment *in vitro* immediately after a 4-h 'uptake' period, and then following 'clearance' phases of 2, 3, 4 and 20 h. Values are the mean and 95% CI (for 'uptake' n = 10 for SC and VT and n = 9 for R; for 'clearance' n = 6, except for 'clearance' 2h in the VT and 'clearance' 20h in the receptor, for which n = 5).
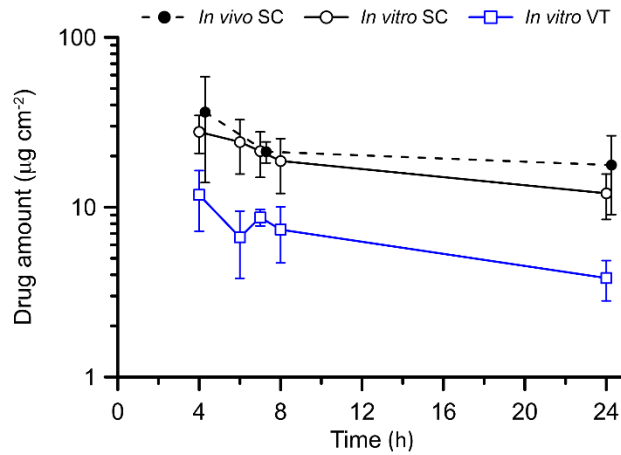
Figure 5. Scopolamine quantities found in the SC *in vitro* and *in vivo*, and in the VT *in vitro*, immediately after a 4-h 'uptake' period, and then following 'clearance' phases of 2, 3, 4 and 20 h *in vitro*, and 3 and 20 h *in vivo*. Values are the mean and 95% CI (*in vivo*, n = 6; *in vitro*, n = 10 for 'uptake' and n = 6 for 'clearance' except n = 5 in the VT at 2 h). To facilitate viewing of the data, the *in vivo* SC results have been shifted slightly to the right by 0.30 h.

Mathematical modeling of IVRT and IVPT experiments

Table 2 summarizes the parameter values derived by best-fit regression of the IVRT and IVPT experimental data to the relevant model. The IVRT data in Figure 2(a) were fitted to Eq. A in Table 1 describing the corresponding model shown in Figure 1. The best-fit regression parameters obtained were $P_0 = 182$ µg cm^{-2}, $\alpha = 0.49$ h^{-1} and $\gamma = 6.4$ µg cm^{-2} h^{-1}; the calculated IVRT curve is shown in Figure 2(a). The corresponding fit to the cumulative drug uptake into the skin and permeated through to the receptor (IVPT model in Figure 1; Eq. C in Table 1 for $M+V+R$), when P_0 was fixed at the value determined in the IVRT experiment, yielded the following best-fit regression parameters: $\alpha = 0.07$ h^{-1} and $\gamma = 5.0$ µg cm^{-2} h^{-1}. These parameters were used in Eqs. B and C to calculate curves for IVPT (R) in Figure 2(a) and IVPT ($M+V+R$) in Figure 3(b). Fitting only the permeation data into the receptor phase (IVPT (R) in Figure 2(a); Eq. B in Table 1) resulted in a minimal change in α (0.10 h^{-1}) and no difference in γ. Fixing P_0 from the IVRT experiment is justified because (i) it is reasonable that the amount of drug delivered from the adhesive should be the same in both the IVRT and IVPT experiments (whereas the rate of drug delivery from the priming dose and the drug reservoir could be different when skin is and is not present); and (ii) a regression fit of the values of $M+V+R$ versus time yields P_0 that is not different from that derived from IVRT.

Assuming the mean drug mass per area in the VT and the SC at 72 h were at steady state, then the rate constants for transfer from the SC to the VT (β) and from the VT to the receptor (δ) during drug uptake, calculated from Eqs. D and E in Table 1, are 1.1 h^{-1} and 0.25 h^{-1}, respectively based on the IVPT γ value of 5.0 µg cm^{-2} h^{-1}. In contrast, β derived by regression to the clearance data collected during 20 h following a 4-h application of the patch is 0.04 h^{-1}, much smaller than for uptake, whereas the clearance and uptake values of δ are similar (0.21 h^{-1} and 0.25 h^{-1}, respectively). The β value derived from the first 4 h of clearance (0.09 h^{-1}) is larger by about a factor of 2 compared with β derived for clearance over 20 h. The total amount of drug in the SC, VT and receptor solution after 4 hours of uptake is equal to $M_{up}+V_{up}+R_{up}$. Based on the IVPT uptake parameter values for α (0.07 h^{-1}) and γ (5.0 h^{-1}), the estimated drug mass transferred from the patch in 4 hours is 64 µg cm^{-2}, which is similar to the sum of the regressed values for M_{up}, V_{up}, and R_{up} and also to the average values of $M+V+R$ for all cells at all clearance times (i.e., 57 µg cm^{-2}).

DISCUSSION

The IVRT data in Figure 2(a) were fitted to Equation (A) in Table 1 describing the corresponding model shown in Figure 1. The best-fit regression parameters obtained were P_0 = 182 µg cm^{-2}, α = 0.49 h^{-1} and γ = 6.4 µg cm^{-2} h^{-1}; the calculated IVRT curve is shown in Figure 2(a). The corresponding fit to the cumulative drug uptake into the skin and permeated through to the receptor (IVPT model in Figure 1; Equation (C) in Table 1 for M+V+R), when P_0 was fixed at the value determined in the IVRT experiment, yielded the following best-fit regression parameters: α = 0.07 h^{-1} and γ = 5.0 µg cm^{-2} h^{-1}. These parameters were used in Equations (B) and (C) to calculate

curves for IVPT (R) in Figure 2(a) and IVPT (M+V+R) in Figure 3(b). Fitting only the permeation data into the receptor phase (IVPT (R) in Figure 2(a); Equation (B) in Table 1) resulted in minimal differences to the value of α (0.10 h^{-1}). Fixing P_0 from the IVRT experiment is justified because (i) it is reasonable that the amount of drug delivered from the adhesive should be the same in both the IVRT and IVPT experiments (whereas the rate of drug delivery from the priming dose and the drug reservoir could be different when skin is and is not present); and (ii) a regression fit of the values of M+V+R versus time yields P_0 that is not different from that derived from IVRT.

The value of γ derived from the IVPT data is reasonably consistent with the Summary of Product Characteristics for the Scopoderm® (1.5 mg) patch [24], which is labelled to deliver 1 mg of drug over 3 days across 2.5 cm^2 of skin, i.e., an average steady rate of 5.6 µg cm^{-2} h^{-1}. From the IVRT and IVPT cumulative permeation and flux profiles in Figure 2, it is evident that the initial delivery of scopolamine – for at least 6 h for IVRT and longer when skin is present – originates from the 'priming' dose in the adhesive. At longer times, drug input to the skin is dominated by the zero-order delivery from the reservoir. Experimentally, the mean total recovery of drug from the receptor and skin tissues at 72 h was 540 µg cm^{-2} (Figure 3(b)). Assuming that the zero-order, 5.0 µg cm^{-2} h^{-1}, delivery of scopolamine to the skin continued over the entire 72 h - accounting for 360 µg cm^{-2} - it follows that drug input from the adhesive 'priming' dose was 180 µg cm^{-2}, in exact agreement with P_0 deduced from the IVRT experiment.

If the patch was able to deliver the same amount of drug at the same rate in both the IVRT and IVPT experiments, then the cumulative amount of drug in the SC, VT and receptor combined should exactly match the cumulative drug released from the patch in the IVRT experiments (i.e., the IVPT (M+V+R) data and curve in Figure 3(b) should overlay the IVRT data and curve).

Clearly, this did not happen. First, more time is needed to release the priming dose when skin is present. This can be understood from the deduction that the time (t_F) required to release a fraction of the priming dose ($F = R/P_0$) can be derived from the IVRT equation (Eq.A in Table 1) for drug mass in the receptor compartment when $\gamma = 0$, i.e.,

$$t_F = -(1/\alpha)\ln(1 - F) \qquad\qquad (2)$$

Hence, specifically, for the IVPT and IVRT α values of 0.07 h^{-1} and 0.49 h^{-1}, it can be estimated that approximately 40 h and 6 h, respectively, are required to release 95% of the priming dose in the IVPT and IVRT experiments. Second, although the steady-state transfer rate (γ) is only a little slower in the IVPT experiment, the difference in the total delivery over 72 h is evident in Figure 3(b). Specifically, by 72 h, after all the priming dose has been delivered, the patch has released almost 100 μg cm^{-2} more drug when skin was absent (IVRT) than when it was present (IVPT ($M+V+R$)).

Figure 6(a) compares the experimental flux data measured from the patch in the absence (IVRT) and presence of skin (IVPT ($M+V+R$)) compared with the model results (J_{patch}) calculated using the P_0, α and γ values listed in Table 2 derived by best-fit to the cumulative drug release from the patch in the IVRT and IVPT-uptake experiments. For the first 6 h, flux from the patch is faster in the IVRT experiment than in IVPT, reflecting the different amounts of the priming dose that has been delivered in each (i.e., most of it in IVRT and less in IVPT). After this, flux from the patch is larger in the IVPT experiment, while the priming dose continues to be delivered, up to the 24-48 hr sampling interval, when the IVPT priming dose is exhausted, and the flux is again slower than IVRT (although not by a statistically significant amount). Figure 6(b) compares the experimental flux data for drug transfer into (IVPT ($M+V+R$)) and out of (IVPT (R)) the skin. The

model prediction for flux out of the skin, $dR/dt = \delta V$, is calculated from the IVPT-uptake equation and parameters (Tables 1 and 2, respectively). After a lag time, drug permeation out of the skin approaches that delivered to the skin.
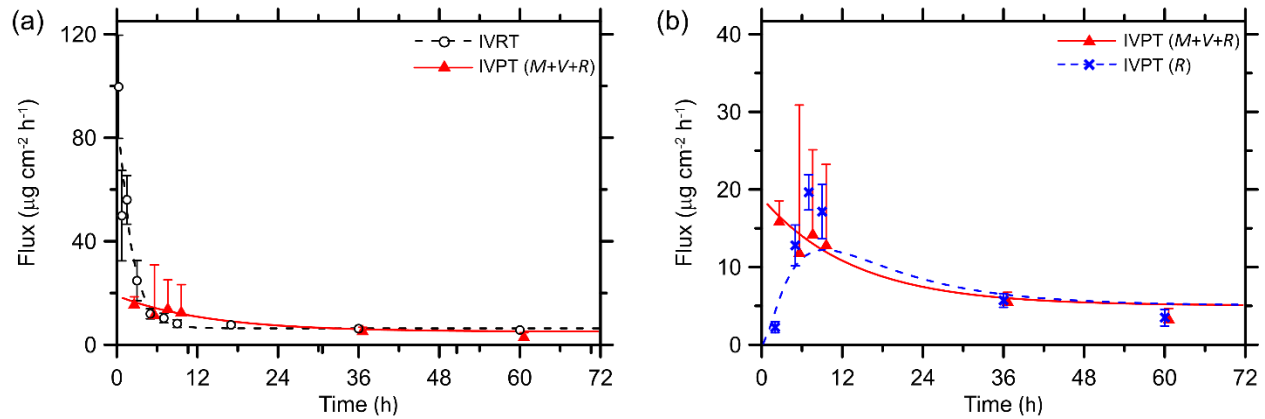

Figure 6. Comparison of the experimental IVRT and IVPT flux data with the best-fit model results: (a) from the patch into the receptor (IVRT) and into the skin (IVPT (M+V+R)), and (b) from the patch into the skin (IVPT (M+V+R)) and from the skin into the receptor IVPT (R). Model parameter values were $P_0 = 182$ µg cm^{-2}; $\alpha = 0.49$ h^{-1} and $\gamma = 6.4$ µg cm^{-2} h^{-1} in the IVRT model; and $\alpha = 0.07$ h^{-1} and $\gamma = 5.0$ µg cm^{-2} h^{-1} for the IVPT model. To facilitate viewing of the data, the IVPT (M+V+R) results have been shifted to the right by 0.60 h.

Although the difference in the IVPT and IVRT steady-state transfer rates (γ) is small, it is enough that drug release to the skin is reduced by 100 µg cm^{-2} compared to release to the receptor in the absence of skin. The additional resistance to drug transfer that occurs when drug release from the patch is measured in the IVPT and IVRT experiments can be estimated from the results. At steady state, with the same driving force, flux from the patch in the IVRT experiment (J_{IVRT}) is about 6.4 µg cm^{-2} h^{-1}, and flux from the patch and through the skin in the IVPT experiment (J_{IVPT}) is ~5.0

26

$\mu g\ cm^{-2}\ h^{-1}$. The steady-state flux through the skin alone in response to the same driving force as the IVRT and IVPT experiments (J_{skin}) is estimated to be 24 $\mu g\ cm^{-2}\ h^{-1}$ using the following expression:

$$\frac{1}{J_{skin}} = \frac{1}{J_{IVPT}} - \frac{1}{J_{IVRT}} \qquad (3)$$

That is, the total resistance of the skin and patch (i.e., $1/J_{IVPT}$) is equal to the sum of the individual resistances for the patch (i.e., $1/J_{IVRT}$) and the skin (i.e., $1/J_{skin}$). Thus, the resistance of transfer through the skin at steady state ($1/24\ \mu g\ cm^{-2}\ h^{-1}$) is approximately 20% of the resistance of drug release from the patch ($1/5\ \mu g\ cm^{-2}\ h^{-1}$). In the IVPT experiments of this study, the patch limits, but does not entirely control, the transfer rate to the skin.

With respect to the priming dose, the initial flux from the patch is $\alpha \cdot P_0$. Because the driving force for transfer of the priming dose to the skin should be the same as for the steady-state flux from the patch, it follows that we can estimate the IVPT rate constant for priming dose release (α_{IVPT}) from the IVRT rate constant for priming dose release (α_{IVRT}) and $1/J_{skin}$ as expressed in Equation (4):

$$\frac{1}{\alpha_{IVPT}} = \frac{1}{\alpha_{IVRT}} + \frac{P_0}{J_{skin}} \qquad (4)$$

For $P_0 = 182\ \mu g\ cm^{-2}$, $\alpha_{IVRT} = 0.49\ h^{-1}$, and $J_{skin} = 24\ \mu g\ cm^{-2}\ h^{-1}$, it follows that $\alpha_{IVPT} = 0.10\ h^{-1}$, which is similar to the 0.07 h^{-1} value estimated by regression to the cumulative transfer from the SC to the skin in the IVPT experiment, and exactly the value estimated by regression to the cumulative transfer from the skin to the receptor solution in the IVPT experiment.

The explanation for the divergence between the IVRT and IVPT (M+V+R) results in Figure 3(b) and the compensatory impact of the 'priming' dose from the adhesive have been discussed in

27

literature published prior to commercialisation of the Scopoderm® product in 1980 [18-20]. Specifically, incorporation of the priming dose into the product aimed to saturate drug immobilization (i.e., binding) sites within the skin [18, 25] and thereby permit more rapid establishment of steady-state plasma levels than were achievable with a system that only comprised the zero-order delivery component of the patch [18].

The IVPT experiments, combined with the assessment of scopolamine levels in the SC and VT as a function of time, provide a comprehensive picture of the local pharmacokinetics of the drug in the skin and of its ultimate transdermal delivery across the barrier. The flux of drug into the receptor phase in IVPT (Figure 2(b)) is a faithful representation of systemic delivery into the blood *in vivo*. Of particular significance, with respect to the overall objective of the present study, is the manner in which the profile of scopolamine disposition in the SC reflects the biphasic delivery profile of the transdermal patch (Figure 3(a)); i.e., the initially rapid input of the 'priming dose' from the adhesive layer followed by the slower, sustained transfer from the reservoir. Notably, the profile in the VT is different and indicates that transfer from the SC is sufficiently slow that a peak is not observed (Figure 3). This is a reflection of the fact that the 'priming' dose is rapidly taken up into the SC, where an important fraction binds tightly [19, 26]; only once the association sites are full can drug be 'released' from the SC to continue its journey towards the systemic circulation.

The clearance experiments were intended to shed further light on the dermatopharmacokinetics. It is observed that clearance from the SC while the patch remains in contact with the skin is slow. In this period, only the 'free', unbound drug is permeating, and the binding sites for scopolamine are presumed to be fully occupied [19, 26]. Upon removal of the patch, the unbound drug clears quickly but that which is bound does not, indicative of a slow and rate-limiting 'off-rate'. This is consistent with the much smaller values for β calculated from the clearance experiments than those

determined from the uptake studies (0.04 h^{-1} compared with 1.11 h^{-1}), whereas values of δ derived from the VT, which has no binding, are not statistically significantly different for the uptake and clearance experiments. With respect to β, it is reasonable to hypothesize that the clearance transfer rate from the SC to the VT is controlled by the scopolamine dissociation kinetics from protein binding. During uptake, the transfer rate from the SC to the VT is controlled by diffusion of only the free (unbound) drug through the tissue. Once the patch, and the drug source, is removed, the continued transfer of unbound drug slows until it is ultimately limited by the rate at which the bound drug dissociates from the binding protein (which is slow). This hypothesis is also consistent with the observed larger clearance rate soon after the patch is removed (approximately two-fold larger in the first 4 h of clearance compared with the entire 20 h) while the unbound drug levels decrease from control by diffusion to control by dissociation.

Figure 7 provides a visual illustration of the complexity introduced by scopolamine binding in the SC as described above. Using the best-fit kinetic parameters of the IVPT-uptake model from Table 2 that adequately describe the cumulative permeation results in Figures 3(b) and the flux results in Figure 6, the SC and VT profiles of scopolamine as a function of time can be predicted using the IVPT-uptake expressions in Table 1 for M and V. Figure 7 compares the model results with the experimental data. It is immediately apparent that, while the sum of the drug levels in the SC + VT are reasonably modelled (at least, at short and long times), those in the SC are significantly under-predicted in the early phase of patch application and those in the VT are over-predicted. The reason for the poor agreement lies, we hypothesize, in the fact that the model used (Figure 1, IVPT) assumes no skin binding and that only unbound drug is present. Further work is therefore required to refine the model to adequately describe the binding mechanisms that are operating.
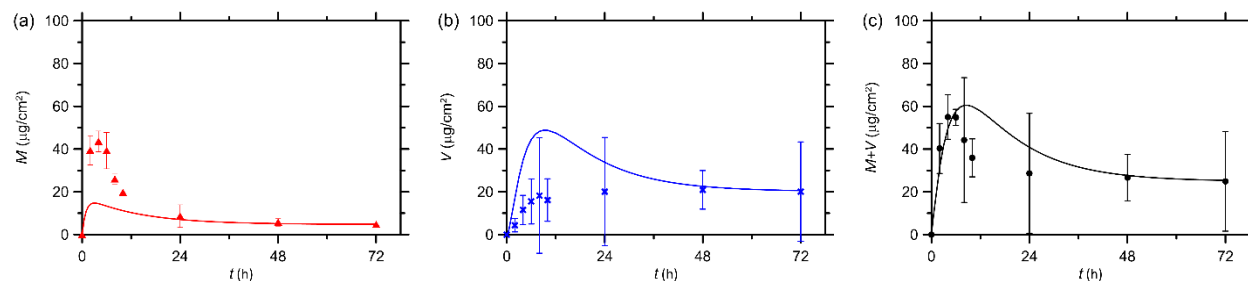
Figure 7. Model predictions of the drug amount per unit area compared to the experimental uptake results acquired *in vitro* in (a) the SC (M), (b) the VT (V), and (c) in the SC and VT combined (M+V). The best-fit parameters used were obtained from fitting the cumulative drug release data from the IVRT measurements in Figure 2(a) (P_0 = 182 μg cm^{-2}) and the IVPT (M+V+R) measurements in Figure 3(b) (α = 0.07 h^{-1}, and γ = 5.0 μg cm^{-2} h^{-1}), and the drug mass in the SC and VT at 72 h assumed to be at steady state (β = 1.1 h^{-1} and δ = 0.25 h^{-1}). Data points represent the mean and 95% confidence interval.

Reversible binding in the SC could be represented by addition of another 'stirred' compartment connected only to SC with rate constants reflecting the forward and reverse processes. This would cause a corresponding increase in the complexity of the IVPT models for the SC and VT compartments. However, determination of parameter values for more complex stirred compartment models can be difficult and is plagued by different combinations of parameter values that produce the same or nearly the same prediction. Although mathematically more complicated, many of the parameters in diffusion models of skin are related to properties that can be determined in independent experiments, thereby reducing the number of parameters that require determination by fitting to the IVPT and/or IVRT data. Thus, diffusion models might be a better choice than stirred compartment models to represent the SC or other skin layers in which additional

mechanisms affect drug transport (e.g., binding). Generally, for estimating drug input to the target compartment, the goal is a model that is only as complicated as needed.

CONCLUSIONS

The central hypothesis examined here is that a relevant and testable physiologically-based pharmacokinetic (PBPK) model can ultimately capture and shed light upon the complex interplay between a topical drug product's attributes and patient outcomes *in vivo*. The development, validation and application of such a model would advance regulatory science and facilitate the design and optimisation of high-quality products for application to the skin. Given that topical drug products are complex, multicomponent systems, the properties of which change profoundly post-application to the skin, drug absorption kinetics are difficult to simulate with a simple mathematical construct. To address this challenge, the drug "input process" to the target tissue beneath the SC must necessarily be characterized experimentally using complementary dermatopharmacokinetic (DPK) techniques. In this way, the kinetic and distribution parameters, which describe the disposition of the drug within the 'black box' between the input from the SC and the systemic blood, can be characterised and ultimately predicted with an appropriate PBPK model. Validation, development and refinement of these strategies for the PBPK modeling and simulation of dermal absorption has, at its core, the goal of a pragmatic approach that is no more complicated than is needed to perform its task. Proof-of-concept has been presented using the known drug "input function" from a transdermal patch, enabling experimental verification, *in vitro* and *in vivo*, of the proposed DPK measurements.

Author Contributions

The manuscript was written through contributions of all authors. All authors have given approval to the final version of the manuscript. The study concept originated with MBDC and RHG. Experimental work was performed by AP; modelling, analysis and statistics by ALB, KAJW, LH and AM. All authors contributed to the final study design, the interpretation of the results and to the writing, review and editing of the manuscript.

Supporting Information. The following files are available free of charge.

Supplementary Figures S1 and S2: File containing **Fig. S1**: *in vivo* tape-stripping study design and **Fig.S2**: Experimental IVPT flux data versus best-fit model results (a) into the SC and VT ($M+V$) from the patch, (b) into the receptor (R) from the skin, and (c) into the SC and receptor ($M+V+R$).

REFERENCES

[1] Yacobi, A.; Shah, V. P.; Bashaw, E. D.; et al. Current Challenges in Bioequivalence, Quality, and Novel Assessment Technologies for Topical Products, *Pharm. Res.* **2014**, 31, 837-46.

[2] Raney, S. G.; Franz, T. J.; Lehman, P. A.; et al. Pharmacokinetics-based Approaches for Bioequivalence Evaluation of Topical Dermatological Drug Products, *Clin. Pharmacokinet.* **2015**, 54, 1095–1106.

[3] Lu, M.; Xing, H.; Chien, X.; et al. Advance in Bioequivalence Assessment of Topical Dermatological Products. *AJPS.* **2012,** 11, 700-707.

[4] Miranda, M.; Cardoso, C.; Vitorino, C. Quality and Equivalence of Topical Products: A Critical Appraisal, *Eur. J. Pharm. Sci.* **2020**, 148, 105082.

[5] Kazem, S.; Linssen, E. C; Gibbs, S. Skin Metabolism Phase I and Phase II Enzymes in Native and Reconstructed Human Skin: a Short Review. *Drug Discov. Today.* 2019, 24,1899–1910.

[6] Nitsche, J. M.; Wang, T. F.; Kasting, G. B. A Two-phase Analysis of Solute Partitioning into the Stratum Sorneum. *J. Pharm. Sci.* **2006**, 95, 649–666.

[7] Hansen, S.; Selzer, D.; Schaefer, U. F.; et al. An Extended Database of Keratin Binding, *J. Pharm. Sci.* **2011**, 100, 1712-1726.

[8] Dancik, Y.; Anissimov, Y. G.; Jepps, O. G.; et al. Convective Transport of Highly Plasma Protein Bound Drugs Facilitates Direct Penetration into Deep Tissues after Topical Application, *BCJP*, **2011**, 73, 564-578.

[9] Kretsos, K.; Miller, M. A.; Zamora-Estrada, G.; et al. Partitioning, Diffusivity and Clearance of Skin Permeants in Mammalian Dermis, *Int. J. Pharm. 2008,* 346, 64-79.

[10] Cheruvu, H. S.; Liu, X.; Grice, J. E.; et al. Modeling Percutaneous Absorption for Successful Drug Discovery and Development, *Expert Opin. Drug Dis.* **2020**, 15, 1181-1198.

[11] Maciel Tabosa, M. A.; Hoppel, M.; Bunge, A.L.; et al. Predicting Topical Drug Clearance from the Skin, *Drug Deliv. Transl. Res*. **2020**, 11, 729–740.

[12] Bravermann, I.M. The Cutaneous Microcirculation, J. Invest. Dermatol. Symposium Proceedings, **2000**, 5, p3-9.

[13] Franz, T. J.; Lehman, P. A.; Raney, S. G. Use of Excised Human Skin to Assess the Bioequivalence of Topical Products, *Skin Pharmacol. Physiol.* **2009**, 22, 276–286.

[14] Pedon de Araujo, T.; Moura Fittipaldi, I.; Galindo Bedor, D. C.; et al. Topical Bio(in)equivalence of Metronidazole Formulations In Vivo. *Int. J. Pharm*. **2018**, 541, 167-172.

[15] Pensado, A.; Chiu, W. S.; Cordery, S. F.; et al. E. Rantou, A.L. Bunge, M.B. Delgado-Charro, R.H. Guy, Stratum Corneum Sampling to Assess Bioequivalence between Topical Acyclovir Products, *Pharm. Res*. **2019**, 36, 180.

[16] Cordery, S. F.; Pensado, A.; Chiu, W. S. et al. Topical Bioavailability of Diclofenac from Locally-Acting, Dermatological Formulations. *Int. J. Pharm*. **2017**, 529, 55-64.

[17] Bodenlenz, M. ; Tiffner, K.; Raml, R.; et al. Open Flow Microperfusion as a Dermal Pharmacokinetic Approach to Evaluate Topical bioequivalence, *Clin. Pharmacokinet*. **2017**, 56, 91–98.

[18] Shaw, J. E.; Chandrasekaran, S. K. Controlled Topical Delivery of Drugs for Systemic Action, *Drug Metab. Rev.,* **1978**, 8, 223-233.

[19] Chandrasekaran, S. K.; Shaw, J. E. Design of Transdermal Therapeutic Systems. In: Contemporary Topics in Polymer Science. Pearce, E. M.; Schaefgen, J. R., Eds.; Springer: New York, 1977, pp. 291-308.

[20] Chandrasekaran, S. K.; Bayne, W.; Shaw, J. E. Pharmacokinetics of Drug Permeation through Human Skin. *J. Pharm. Sci.***1978**, 67, 1370-1374.

[21] N'Dri-Stempfer, B.; Navidi, W. C.; Guy, R. H.; et al. Improved Bioequivalence Assessment of Topical Dermatological Drug Products Using Dermatopharmacokinetics. *Pharm. Res*. **2009**, 26, 316-328.

[22] Kalia, Y.N.; Pirot, F.; Guy, R. H.; Homogeneous Transport in a Heterogeneous Membrane: Water Diffusion across Human Stratum Corneum In Vivo. *Biophys. J.* **1996**, 71, 2692-2700.

[23] Kalia, Y. N.; Alberti, I.; Sekkat, N.; et al. Normalization of Stratum Corneum Barrier Function and Transepidermal Water Loss In Vivo. *Pharm. Res*. **2000**, 17, 1148-1150.

[24] Electronic Medicines Compendium (emc), Scopoderm 1.5 mg Patch, SmPC, https://www.medicines.org.uk/emc/medicine/29044#gref (accessed 8 March 2021)

[25] Shaw, J. E. Transdermal Dosage Forms, *Meth. Enzymol*. **1985**, 112, 448-461.

[26] Urquhart, J.; Chandrasekaran, S. K.; Shaw, J. E. 1977. Bandage for transdermally administering scopolamine to prevent nausea, US 4,031,894, June 28.

SUPPLEMENTARY INFORMATION

Skin pharmacokinetics of transdermal scopolamine: measurements and modelling

Andrea Pensado[1,*], Laura Hattam[2], K.A. Jane White[3], Anita McGrogan[1], Annette L. Bunge[4],

Richard H. Guy[1], M. Begoña Delgado-Charro[1,*]

[1] Department of Pharmacy & Pharmacology, University of Bath, Bath, BA2 7AY, UK

[2] Institute for Mathematical Innovation, University of Bath, Bath, BA2 7AY, UK

[3] Department of Mathematical Sciences, University of Bath, Bath, BA2 7AY, UK

[4] Chemical and Biological Engineering, Colorado School of Mines, Golden, Colorado, 80401, USA
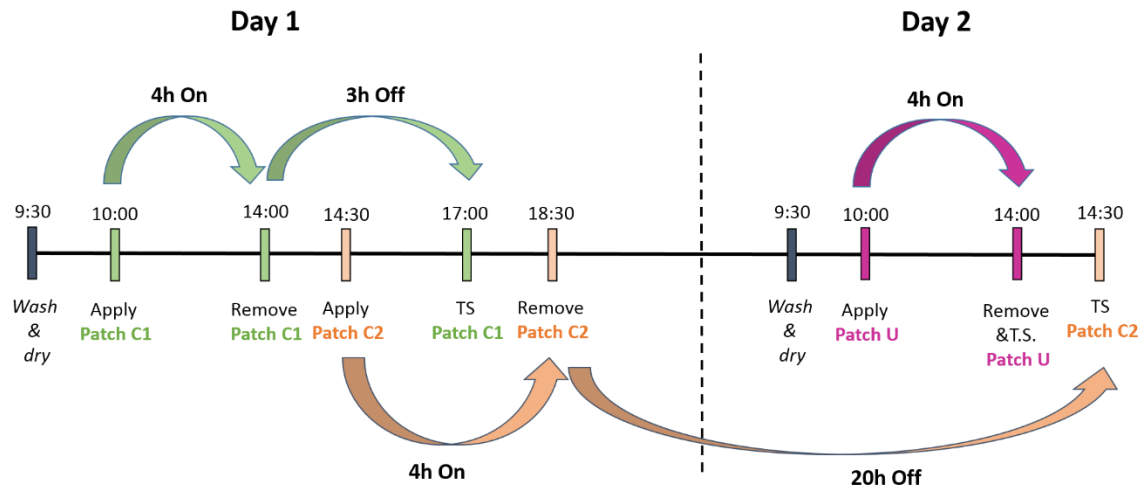
SUPPLEMENTARY INFORMATION

Figure S1: *In vivo* tape-stripping study design showing illustrative timings of patch application and removal (all with an 'uptake' time of 4 h) and the subsequent times at which SC sampling was performed: immediately for Patch U, and after 'clearance' times of 3 h and 20 h for patches C1 and C2, respectively.

Figure S2 shows the scopolamine flux into the SC and VT combined ($M+V$), into the receptor (R), and into the skin and receptor combined ($M+V+R$) compared with model predictions that used parameters derived by regression to the cumulative drug release data from the IVRT and the IVPT ($M+V+R$) measurements. Data are plotted as the mean and 95% confidence interval, which was calculated using the two-tailed Student's t-distribution of a probability of 0.05 for the sample size and standard deviation. Flux is plotted at the mid-point of the sampling times in the time interval.

The drug mass per diffusion area was measured in both the SC and VT ($M+V$) at 4, 6, 8, 10, 24, 48 and 72 h in three skin samples (except at 4 h, which was measured in 9 samples). The $M+V$ flux was calculated from the mean value of the drug mass per area at successive sampling time points divided by the time interval between the sampling times. The confidence intervals of the $M+V$ flux, plotted in Figure S2(a), were calculated using the standard deviation estimated by pooling the standard deviations of the $M+V$ drug amounts at the beginning and end of the flux time interval, and n = 3, except for the flux at 2 h, which was calculated from measurements at 4 h (n = 9) compared to no drug at 0 h.

Drug amounts in the receptor (R) were measured at as few as 2 or as many as 5 of 8 sampling time points (2, 4, 6, 8, 10, 24, 48 and 72 h) in each of 22 diffusion cells experiments. Flux into the receptor was calculated for each experiment with measurements at the beginning and end time points of 6 time intervals (0-4, 4-6, 6-8, 8-10, 24-48, and 48-72 h). Flux was not calculated for the $10^{-}24$ h interval because the drug masses at 10 and 24 h were not both measured in any experiment. The 95% confidence intervals in Figure S2(b) were calculated in the usual way from the number and the standard deviation of the replicated flux measurements for each time interval; at 2 h (n = 22), 5 h (n = 14), 7 h (n = 6), 9 and 60 h (n = 3) and 36 h (n = 4).

The flux into the skin and receptor combined ($M+V+R$) at each time point in Figure S2(c) was calculated from the sum of the mean values of the $M+V$ flux and the R flux at that time. The confidence intervals for each data point were estimated from the sum of the variance for the flux into R and the variance for $M+V$ flux (which pooled the standard deviations from measurements at the beginning and end of the sampling interval). We used this approach because the $M+V$ flux and the R flux are independent measurements. The reported confidence intervals were estimated using the smaller of the sample sizes for the R flux and the $M+V$ flux, which were generally not the same; this gave n = 3 at all time points except 2 h (n = 9).
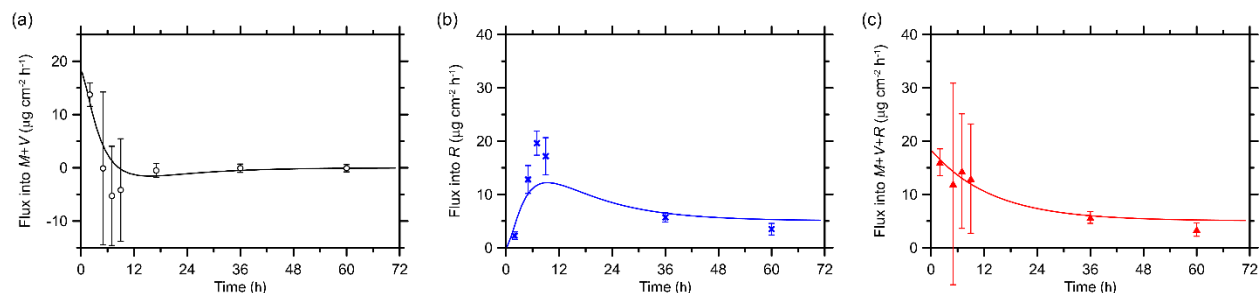

Figure S2. Comparison of the experimental IVPT flux data with the best-fit model results (a) into the SC and VT ($M+V$) from the patch, (b) into the receptor (R) from the skin, and (c) into the SC and receptor ($M+V+R$). The best-fit parameters used were obtained from fitting the mean values of the cumulative drug release data from the IVRT measurements in Figure 2(a) ($P_0 = 182$ µg cm^{-2}) and from the IVPT ($M+V+R$) measurements in Figure 3(b) ($\alpha = 0.07$ h^{-1}, and $\gamma = 5.0$ µg cm^{-2} h^{-1}). Data points represent the mean and 95% confidence interval, which were estimated as described in the text.